Polyurethane Shape Memory Filament Yarns: Melt Spinning, Carbon-based Reinforcement and Characterization

Judit González[1,2,3], Mònica Ardanuy[1], Marta González[3], Rosa Rodriguez[2] and Petar Jovančić[2,4]

[1] Departament de Ciència i Enginyeria de Materials (CEM), Universitat Politècnica de Catalunya (UPC), Terrassa 08222, Spain

[2] Eurecat, Centre Tecnológic de Catalunya, Unitat de Teixits Funcionals, Av. d'Ernest Lluch 36, Mataró, 08302, Spain

[3] Elisava Barcelona School of Design and Engineering, Barcelona, 08002, Spain

[4] Textile Engineering Department, Faculty of Technology and Metallurgy, University of Belgrade, Karnegijeva 4, 11120, Belgrade, Serbia

ABSTRACT

The aim of this work was to develop and characterize polyurethane-based shape memory polymer (SMPU) filament yarns of a suitable diameter and thermo-mechanical performance for use in tailored multi-sectorial applications. Different polymer compositions - pure SMPU and SMPU composites with 0.3 and 0.5 wt.% of multi-walled carbon nanotubes (MWCNT) or carbon black (CB) as additives - were studied.

Filaments were obtained using a melt spinning process that allowed the production of the permanent and temporary shape of the SMPU filament. Two drawing speeds (20 and 32 m/min) were studied.

Characterization techniques such as the tensile test, differential scanning calorimetry (DSC) and dynamic mechanical analysis (DMA) were used to investigate the shape-memory effect (SME) of the filaments.

Pure and additive SMPU filament yarns of a controlled diameter were produced. The results indicated that the pure SMPU on the temporary shape had the highest tensile strength (234MPa). Filaments with CB revealed a significant strain (335%) in the permanent shape with respect to the other filaments. The melt spinning process influenced the soft segment glass transition temperature (T_{gs}) significantly, with a decrease in the temporary shape (1st heating) as compared to the permanent shape (2nd and 3rd heating). However, only the 0.5% MWCNT additive clearly influenced the filament, increasing the T_{gs} by 10ºC. The additives also influenced the SME, obtaining an increased fixity ratio (up to 97%) with the MWCNT additive and an increased recovery ratio (up to 86%) with the CB additive.

Key works: *SMPU, filament yarn, mechanical properties, thermal properties, recovery ratio, fixity ratio, permanent shape, temporary shape.*

INTRODUCTION

Shape Memory Polyurethanes (SMPUs) can recover a programmed or permanent shape from a deformed or temporary shape. This functionality is sensitive to external stimuli such as heat, light, or humidity. Temporary shape fixity and recovery to the permanent shape are related to the SMPU's capacity to produce the shape memory effect (SME). These properties depend on the SMPU filament processing parameters, such as thermal conditions and applied mechanical deformation.[1]

According to Baer et al. (2007),[2] SMPUs are segmented polyurethanes having a microphase configuration. They are divided into hard segments (aromatic diisocyanates), which generate the permanent shape and are responsible for shape recovery; and soft segments (aliphatic polyethers or polyesters), which create the temporary shape and are responsible for shape fixity. The shape memory effect (SME) of these SMPUs is produced by the thermodynamic incompatibility between the hard and soft segments.[3] Depending on the formulation, transitions may be located at the

melting temperature (T_m) or the glass transition temperature (T_g) of the hard segment (T_{mh} or T_{gh}, respectively), and at the T_m or T_g of the soft segment (T_{ms} or T_{gs}, respectively).[4] When stress is generated in the tensile direction, the deformation, in the form of the orientation of the polymer chains, is stored elastically in the soft segment, while the hard segment remains virtually unchanged. In order to obtain the effective functionality of the SMPU, attractions between the polymer chains of the hard segments must be maintained in the presence of stress, while the soft segment absorbs said stress and lengthens its chains.[5]

Figure 1 shows a scheme of the process undergone to create the permanent shape, the temporary shape and to recover the permanent shape for an SMPU filament.

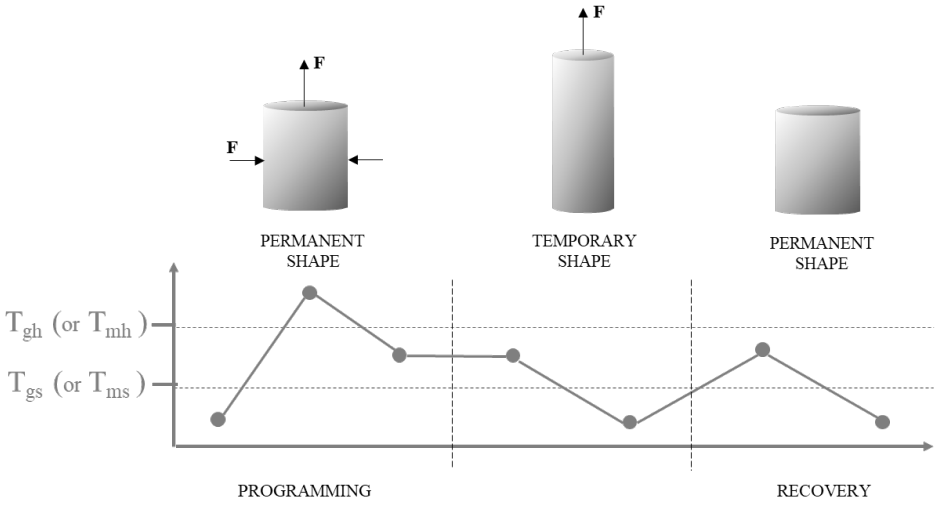

Figure 1. Scheme of the transition temperatures from de creation the permanent shape, the change to the temporary shape and the permanent shape recovery of an SMPU filament.

Different studies focus on the development of new shape memory polymers with improved performance, modifying their composition or including additives. A variety of additives have been studied and used to strengthen SMPUs (organic clay, carbon nanofibers (CNF), silicon carbide (SiC), carbon black (CB), carbon nanoparticles/tubes/wires, graphene and silver nanoparticles (AgNP) /nanowires (AgNW)).[6,7] However, many studies have focused on the effects of CB and carbon nanotubes (MWCNT), proving to be stable and effective additives.[3,8–12] MWCNT are tubular 1D nanomaterials, while CB are spherical nano or microparticles. Their distinct morphologies result in different effects on the SMPU segments. According to Meng and Hu[9], MWCNT can lead to an improvement in temporary shape recovery and stress recovery that is higher than CB. These additives can affect the crystallization of the soft segments of the SMPU, restricting their mobility in different ways, depending on the size of the additives. These findings suggest that SMPU properties are influenced by the presence of additives and that, depending on their distribution in the matrix, as well as their nature, morphology and content, they may have distinct effects which require further study. Some works have suggested that a variation in geometry and particle size may cause an increase or decrease in the T_{gs} of the SMP.[10]

It has been found that additive contents above 1wt.% result in filaments having unsuitable diameter and mechanical performance for multi-sectorial applications.[3,13–16] Although numerous studies have considered the

incorporation of additives (CB and MWCNT) in SMPU, none have analyzed the mechanical and dynamic-mechanical behavior of filaments containing less than 1% of these additives. [7,9,13–21,22–24]

Of the industrial processes used to create SMPU masterbatches with nanoparticles, the most common are ultrasonication-assisted solution mixing, shear mixing, three roll milling, ball milling and co-rotating twin screw.[25] Of these, the most energy-efficient and suitable for industrial production is co-rotating twin screw extrusion.

On the other hand there are many spinning methods among them: bubble spinning, electrospinning, dry spinning, wet spinning, chemical and melt spinning.[3,26,27] There are some studies have analyzed the effect of production processes,[28] such as production through electrospinning,[29] melt spinning or wet spinning, on the mechanical performance and shape recovery[2] of SMPU in the form of fibers or thin films.[30] However, melt spinning is considered the most appropriate for industrial production .[31]

Other research has focused on the effect of thermal treatments on the filaments.[32,33] According to Kaursoin et al.[12], heat-setting and drawing affect shape memory effect properties. Finally, a limited number of studies have analyzed the viability of the applications of the shape memory fibers on knitted fabrics.[34–37]

This study, using a melt spinning process, aims to obtain SMPU filament yarns having a suitable diameter for multi-sectorial applications by incorporating a low percentage of additives (0.3 and 0.5 wt.%) through a co-rotating twin-screw extrusion. The incorporation of these additives will result in a wide range of filaments with distinct properties. Thus, it is intended to expand the range of SMPU filament yarns for use in different applications.

The co-rotating twin screw method was selected for the masterbatch preparation since micro and nanoscale additives permit further industrial use. Several studies have obtained positive dispersing results using this method.[4,38,39] According to previous studies, it is expected that additives at this low content will permit the production of regular filament yarns that are appropriate for multi-sectorial applications and which may contribute to differences in mechanical and thermomechanical behavior and shape memory behaviour.[14,40]

The melt-spinning process is expected to partially orient the polyurethane molecules in the direction of the fiber axis and thereby, form hard segment microdomains. This may lead to a higher fiber breaking strength as compared to other formats.[30,41] This orientation will increase with drawing speed.[3]

The influence of the melt-spinning and drawing speed process parameters, as well as the effect of the incorporation of MWCNT and CB on the diameter, mechanical performance, thermal properties, and SME behavior of the filament yarns on temporary and permanent shapes were examined. SME behavior was assessed by determining the fixity ratio of the temporary shape and the recovery ratio for the return to the permanent shape.

Materials and experimental methods

MATERIALS

The polymer used was an SMPU, ether-based polyurethane (MM4520 grade) having an activation temperature of 45ºC, provided by SMP Technologies Inc., Japan. To program the SMPU, it was necessary to heat the polymer above the T_{gh}. Once the material acquired the desired shape (the so-called *permanent shape*), it was maintained at

temperatures above the T_{gs}. The deformed shape (the so-called *temporary shape*) was achieved by applying stress and cooling the material below the T_{gs}.[42]

Multi-walled carbon nanotubes (MWCNT) MWNC7000™ series (from NANOCYL, Belgium) and carbon black (CB) in microparticles made up of nano-sized carbon filaments with accessible pore structure were used as received.

EXPERIMENTAL METHODS

Preparation of SMPU composites

Additivation was carried out with a ZSK 18 MEGAlab co-rotating twin screw extruder equipped with two hoppers. Detailed information on the method used in this study was presented by Uranbey et al.[39] First, a masterbatch of SMPU containing 3 wt.% of MWCNT or CB was prepared. This masterbatch was proportionally blended with pure SMPU (SMP45P-P) in another extrusion process, to attain values of 0.3 and 0.5 wt.%, for MWCNT and CB particles. The temperature profile of the extruder ranged from 180 to 220°C for MWCNT and from 180 to 210°C for CB, to ensure a homogeneous mixture with no polymer degradation. The SMPU pellets and masterbatch were dried at 80ºC for 4 hours, or until the humidity percentage was less than 0.03%, before extrusion. The following formulations were prepared: SMP45P-MWCNT03 (0.3 wt.% of MWCNT); SMP45P-MWCNT05 (0.5 wt.% of MWCNT); SMP45P-CB03 (0.3 wt.% of CB); and SMP45P-CB05 (0.5 wt.% of CB). The effect of the CB or MWCNT on polymer viscosity was determined with the Melt Flow Rate (MFR) at 190ºC.

Melt spinning process

Pure SMPU and composite pellets were melt-spun with a Collin Tech-Line extruder followed by a first drawing zone (stretching roller A), a hot-air stretching furnace and a second drawing zone (stretching roller B), as seen in Figure 2.

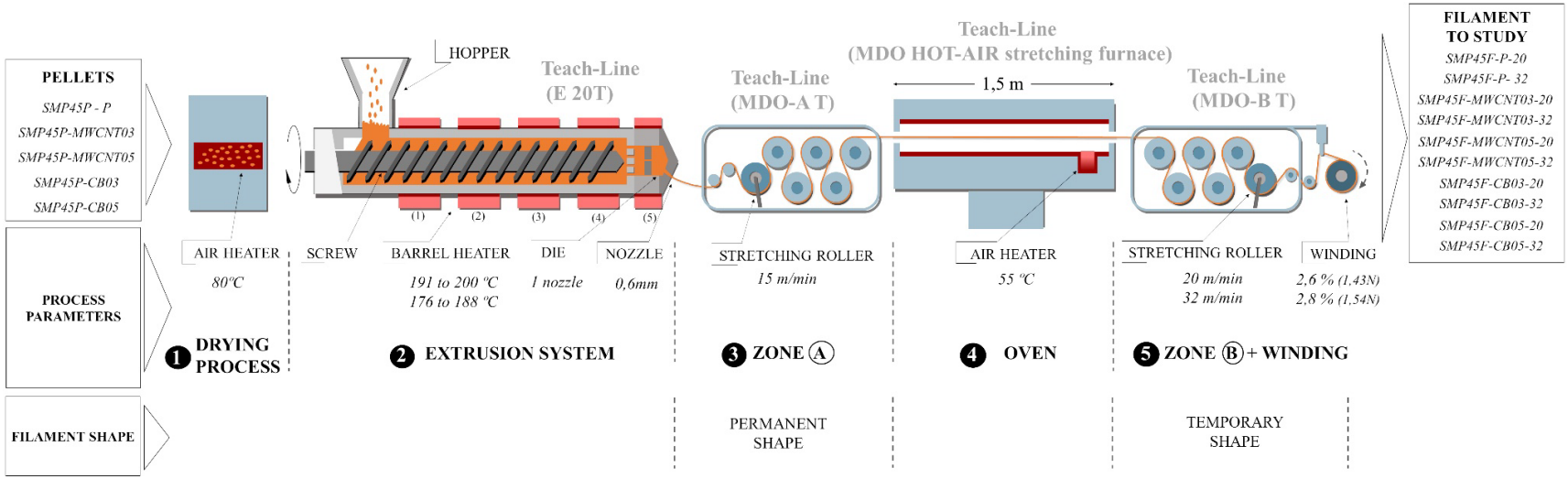

Figure 2. Scheme summarizing the process used for filament manufacture and study.

The main parameters of the process are indicated in Figure 2, as well as the pellets used and the monofilament yarns (referred to as *filaments* in this paper) obtained. The nomenclature includes the name of the polymer (SMP45), the form (P-pellet or F-filament), the additives (CB or MWCNT), the content of the additive (0.3 or 0.5 wt.%), and the stretching speeds (20 or 32 mm/min). Additionally, two percentages of CB (0.1 and 1 wt.%) were added.

A 0.6 mm diameter nozzle was used to obtain filaments with an adequate diameter for multi-sectorial applications. Temperature ranges and other parameters of the extrusion process were adjusted, depending on the viscosity of the pellets used (pure SMPU or composites)[4] and the results of Melt Flow Rate (MFR) shown in Table 1. The MFR of the SMPU filaments were examined using a CEAST melt flow modular line indexer (ITALY) at 190°C.

Table 1. Melt Flow Rate (MFR) values of the different formulations.

SAMPLE NOMENCLATURE	MFR (g/10 min)
SMP45P-P	8.39 ± 1.05
SMP45P-CB03	31.08 ± 0.73
SMP45P-CB05	30.03 ± 0.97
SMP45P-MWCNT03	43.22 ± 1.35
SMP45P-MWCNT05	26.21 ± 0.86

As observed by previous authors,[10] a significant reduction was found in SMPU viscosity due to the effect of the additives, having a three to five-fold higher flow rate (from 26 to 43 g/min) as compared to pure SMPU (approximately 8g/10min). Based on these MFR values, the extruder temperature was approximately 15ºC lower for the composites as compared to the pure SMPU.

The programed filament shape (referred to as the *permanent shape* in this paper) was created by cooling at $<T_{gh}$ once the material extrusion was carried out at the fixed drawing speed of 15 m/min (Zone A). To produce a deformed shape (referred to as a *temporary shape* in this paper) during this extrusion process, the filaments were passed through a 1.5m long furnace placed between Zone A and Zone B. As in previous studies,[4,11,42–44] the oven temperature was fixed at 55ºC, that is, above the T_{gs} of all of the SMPU filaments. To continuously control the final SMPU filament diameter (yarn count) and the thermo-mechanical properties of the same, two different drawing speeds (20 m/min or 32 m/min) were applied in Zone B. Our previous work clearly indicated that the selected drawing speeds permit a very stable extrusion process with production relevance for a significant quantity of SMPU filaments.

To return to the permanent shape, filaments were heated above the T_{gs} without the application of any external stress. During this process, the internal stresses generated during the extruding process (and stored in the temporary shape) were erased, permitting the return to the permanent shape.[43]

Characterization techniques

Filament diameters were measured in the temporary and the permanent shape (after heating to 60 °C), using a high accuracy digital micrometer (Mitutoyo 293 series), enabling 0.1 µm (micrometer) resolution measurements. To

determine the average filament diameter, single measurements were taken at every 25 cm on 10 m filament lengths (different filament samples were used to obtain the average filament diameter value with a 95% confidence interval).

Tensile tests were performed according to ISO-2062:2009 standards, using a ZwickRoell static testing machine. Twenty (20) specimens of 125 mm length were tested for each formulation. Pre-tension was applied according to filament diameter and the displacement rate of 25 mm/min. The test was performed on the filaments after the spinning and drawing (on the temporary shape). It was carried out on the filaments after spinning and drawing, followed by heating to 60ºC (on the permanent shape).

The thermal transitions of the materials were determined by differential scanning calorimetry (DSC) over a temperature range (between 25 and 250ºC), using a heating rate of 20ºC/min. Three heating and cooling cycles were run for each material. The materials were analyzed in pellet form on a DSC 822e Mettler machine and filaments were analyzed using a DSC Q20 V24.11 Build 124 (TA Instrument). Thermal gravimetric analysis (TGA) was conducted on a TGA/SDTA 861 Mettler machine at a heating rate of 20ºC/min in the 50ºC to 800ºC temperature range and in a nitrogen atmosphere (60 ml/min), for pure SMPU. The composites were analyzed in the 50°C to 650°C range in a nitrogen atmosphere (60 ml/min) and from 650ºC to 1000°C in an oxygen atmosphere (60 ml/min). Both samples were in pellet form.

To determine the shape memory effect (SME), i.e., the stability of the temporary shape, fixity ratio (R_f), and the recovery of the permanent shape -recovery ratio (R_r)-, Dynamic Mechanical Analyses (DMA) were performed on a DMA Q800 by TA Instruments. Two types of tests were carried out. The aim of the first test was to determine the minimum reference temperature required to erase the memory form of the temporary shape. Three (3) specimens of 16 cm ±0.3 in length were subjected to tensile deformation at a temperature range of 20°C to 100°C at 3°C/min and 1Hz for each composition. The transition temperature (T_{gs}) and transition modulus were obtained for each specimen. For all of the specimens, a reference temperature (T_r) was determined using the highest value of T_{gs}.

The second test was used to determine the SME of the filaments. Tests were performed on 10 mm ±0.5 length filaments. The following test steps were used: first, the samples were heated to T_r at a heating rate of 3ºC/min. After maintaining T_r for 1 min, a force ramp of 0.01 N/min was applied, to achieve a maximum strain (ε_m) of 100%. Then, the force was maintained while the sample was cooled to 27°C, maintaining this temperature for 15 min. Next, the sample was stored at T_r, without applying any force, for 5 min. Without this force, a recovery of strain (ε_u) occurred. The process ended when the sample was once again heated to T_r, producing a residual deformation (ε_p). This final measure was the start of the next cycle. This cycle was repeated 3 times for each specimen and after each cycle, the recovery length was measured. The shape fixity ratio (R_f) and shape recovery ratio (R_r) were determined from these data tests. The R_f is related to the soft segment of the PU and the R_r is related to the hard segment.[12,42,45] Recovery and fixity rates were calculated with the following equations (1) and (2)[42,44]:

$$R_r\ (\%) = \frac{\varepsilon_m - \varepsilon_p}{\varepsilon_m} \times 100 \qquad (1)$$

$$R_f\ (\%) = \frac{\varepsilon_u}{\varepsilon_m} \times 100 \qquad (2)$$

All of the results obtained were statistically treated with an analysis of variance (ANOVA) and the Tukey HSD test using SAS GLM software, providing the significance groups for the same.

Results and discussion

Diameter of the filaments

The diameter and length of the filaments were measured. The sample nomenclature, process parameters and diameters of the filaments obtained in the temporary and permanent shapes are presented in Table 2.

Table 2. Sample nomenclature, main parameters of the spinning process and the filament diameters obtained.

	MAIN PARAMETERS OF SPINNING PROCESS		FILAMENT TEMPORARY SHAPE		FILAMENT PERMANENT SHAPE	
SAMPLE NOMENCLATURE Units	BARREL HEATER PROFILE (1-5) (ºC)	ZONE B SPEED (m/min)	AVERAGE DIAMETER (µm)	LINEAR DENSITY (dtex)	AVERAGE DIAMETER (µm)	LINEAR DENSITY (dtex)
SMP45F-P- 20	191-200	20	219±17	480	311±12	820
SMP45F-P- 32	191-200	32	172±10	360	303±11	840
SMP45F-MWCNT03-20	178-186	20	240±13	560	288±14	840
SMP45F-MWCNT03-32	178-186	32	176±17	260	279±13	780
SMP45F-MWCNT05-20	176-183	20	290±26	860	370±13	1380
SMP45F-MWCNT05-32	176-183	32	247±10	630	369±8	1320
SMP45F-CB03-20	177-185	20	227±12	500	284±14	740
SMP45F-CB03-32	177-185	32	167±16	270	260±13	730
SMP45F-CB05-20	179-188	20	249±17	490	296±8	830
SMP45F-CB05-32	179-188	32	215±20	320	307±16	900

As shown in Table 2, the melt-spun filaments on the temporary shape had cross-sectional diameters ranging between 167 and 290 µm (with a linear density between 260 and 860 dtex) and between 260 and 370 µm for the permanent shape (linear density between 730 and 1380 dtex). The results of the diameter measurements were statistically analyzed and indicated that smaller than average diameters were obtained for higher drawing speeds. According to the Tukey test, the differences found were significant.

For the filaments on the temporary shape, an increase in diameter was found with the addition of CB and MWCNT. This value was higher for SMP45F-MWCNT05-20. The Tukey test revealed significant differences in additives with 0.5 wt.% MWCNT as compared to the other filaments. This behavior could be related to the effect of the additive in the microstructure formed during the crystallization process.[9]

As for the diameter variation in the recovery from the temporary to the permanent shape, in most of the cases, it was found that filaments with a drawing speed of 20 m/min had a lower recovery percentage, between 44-62%, as compared to filaments with a drawing speed of 32 m/min (Table 3). The Tukey test revealed significant differences between the groups having different drawing speeds. SMP45F-P-32 had the highest diameter recovery (76%). The Tukey test confirmed that this difference in recovery was significant for all filament types. This behavior was attributed to the influence of additives on molecular orientation during extrusion. Therefore, it was considered that CB produced a

restriction effect on the mobility and orientation of the soft segments of the SMPU during crystallization, while MWCNT acted as a nucleating agent.[3,9]

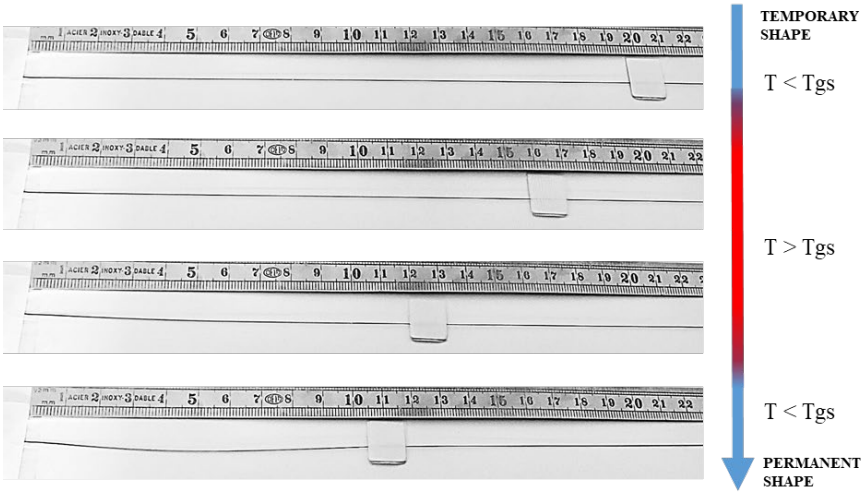

Figure 3. Recovery process of the temporary to permanent shape for the SMP45F-CB03-32 filament

As for the length recovery from temporary to permanent shape (Figure 3), in most of the filaments, the length was recovered in a similar percentage as the diameter (with a 4-12% difference between these recoveries) (Table 3). An exception was found for the SMP45F-CB05 which, according to the Tukey test, revealed a significant difference of 17-18% in recovery between the length and the diameter. This may be due to the influence of particle size and geometry combined with the molecular orientation, on the direction of the length, produced by the extrusion process.[3,10]

Table 3. Percentages of diameter and length recovery of the filaments from temporary to permanent shape

	RECOVERY TO PERMANENT SHAPE	
SAMPLE NOMENCLATURE	**DIAMETER**	**LENGTH**
Units	**(%)**	**(%)**
SMP45F-P- 20	42 ±4.1	49 ±1.8
SMP45F-P- 32	76 ±5.6	67 ±0.8
SMP45F-MWCNT03-20	20 ±4.3	27 ±1.9
SMP45F-MWCNT03-32	58 ±4.0	52 ±1.4
SMP45F-MWCNT05-20	25 ±5.0	40 ±1.1
SMP45F-MWCNT05-32	56 ±6.1	55 ±0.7
SMP45F-CB03-20	27 ±2.8	36 ±1.2
SMP45F-CB03-32	49 ±3.4	51 ±2.0
SMP45F-CB05-20	19 ±3.1	36 ±2.6
SMP45F-CB05-32	43 ±5.4	61 ±1.8

Differences between diameter and length recovery for the different filaments permit the refining of a range of shape memory behaviors for different applications. Therefore, a higher or lower recovery percentage for diameter or length could have distinct functionalities. For example, filaments could be designed for specific applications requiring high diameter recovery but low length recovery, or high or low recovery in both directions, etc.

Mechanical performance

Figure 4 shows the representative tensile strength-strain curves obtained for the filaments on temporary and permanent shapes from the tensile tests. The values of maximum strength and strain are summarized in Table 4.

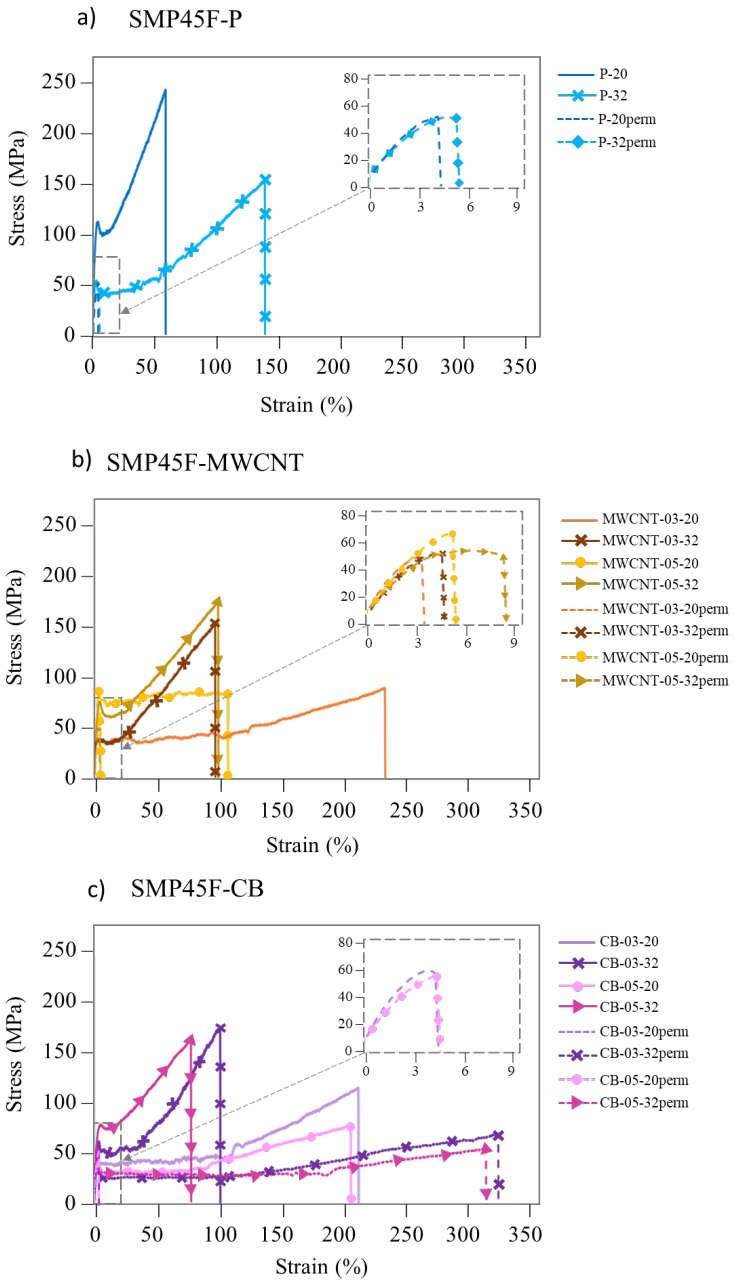

Figure 4. Stress–strain representative curves in static tensile tests of the SMPU filaments obtained for temporary shapes (solid colors) and permanent shapes (stripes) for: a) pure SMP45F-P filaments; b) composite filaments with SMP45F-MWCNT and c) composite filaments with SMP45F-CB.

As expected, the filaments on the temporary shape produced at the highest drawing speed (32 mm/min) had higher tensile strengths than those produced at 20 mm/min. This effect was more noticeable with the composite filaments.[3,30] According to the Tukey tests, these differences were significant for all filament types.

As for the effect of the additives, a decreased tensile strength was found, as compared to the pure polymer which reached the highest average (234 MPa) (Table 4). The Tukey test indicated that differences between pure SMPU filaments and composites were significant. These tests also indicated that no significant differences in tensile strength were found between additives, with the SMP45F-CB03-32 reaching the highest average tensile strength (182 MPa) of the composites.

This behavior is the opposite of that observed by Miaudet et al.[46] who found that additives doubled the tensile strength value of the pure polymer. This difference in behavior could be related to the significantly lower quantity of the additives in this study (0.3 and 0.5 wt.%) as compared to those of the study by Miaudet et al. (20 wt.%). Or it may be a result of the distinct polymer and filament production process.

Table 4. Maximum tensile strength and strain values obtained from the tensile tests for all filaments on temporary and permanent shapes.

	TEMPORARY SHAPE		PERMANENT SHAPE	
SAMPLE NOMENCLATURE **Units**	**MAX. STRENGTH (MPa)**	**MAX. STRAIN (%)**	**MAX. STRENGTH (MPa)**	**MAX. STRAIN (%)**
SMP45F-P- 20	168 ±23	149 ±24	52 ±3	6 ±1
SMP45F-P- 32	236 ±30	59 ±12	47 ±4	4 ±0
SMP45F-MWCNT03-20	94 ±12	239 ±20	49 ±5	4 ±1
SMP45F-MWCNT03-32	160 ±35	96 ±27	52 ±6	4 ±1
SMP45F-MWCNT05-20	93 ±19	116 ±29	63 ±9	5 ±3
SMP45F-MWCNT05-32	177 ±21	100 ±9	53 ±3	8 ±4
SMP45F-CB03-20	118 ±8	216 ±11	48 ±5	5 ±1
SMP45F-CB03-32	182 ±31	96 ±25	68 ±10	306 ±38
SMP45F-CB05-20	81 ±12	202 ±19	56 ±5	5 ±1
SMP45F-CB05-32	160 ±29	71 ±16	57 ±9	335 ±37

The filaments on the permanent shape had a lower tensile strength (47-68 MPa) as compared to those on the temporary shape. Higher values were observed for the composite filaments, although according to the Tukey test, these differences were not significant. This effect was more noticeable for composites with a higher additive content. This may be due to the more restricted mobility of the soft segments of the SMPU and the effect of the particles.[3,8,10–12,47]

Given that the addition of a low amount of CB and MWCNT led to filaments having a more similar tensile strength in both temporary and permanent shapes than the pure polymer, applications may be designed in which a homogeneous tensile strength is useful for the temporary and permanent shapes. On the other hand, pure filaments may be suitable for applications requiring extensive strength on the temporary shape.

The filaments on the temporary shape at 20m/min drawing speed revealed higher strain values than those produced at 32m/min. Moreover, in most of the filaments, the composites presented higher strain than the pure SMPU at the same drawing speed, with the SMP45F-MWCNT03-20 revealing the highest strain (239%) and the SMP45F-P-32

filament having the lowest strain (58%). These differences between pure SMPU and composites were significant according to the Tukey test. This may be due to the higher tensile strength of the pure material, as compared to that of the composites.

On the other hand, most of the filaments on the permanent shape had lower strain values and lower strength than those on the temporary shape. According to the Tukey test, these differences were significant. This expected behavior is related to the increase in molecular orientation and tensile strength resulting from the drawing of the filaments to produce the temporary shape.[10,48,49] This happens in all the materials except for the composites with CB, which had a very high strain (335%).

To confirm these findings, filaments containing 0.1 wt.% and 1 wt.% of CB, SMP45F-CB01 and SMP45F-CB1, respectively, were also produced. In both cases, results showed that the same effect occurred (Figure 5).

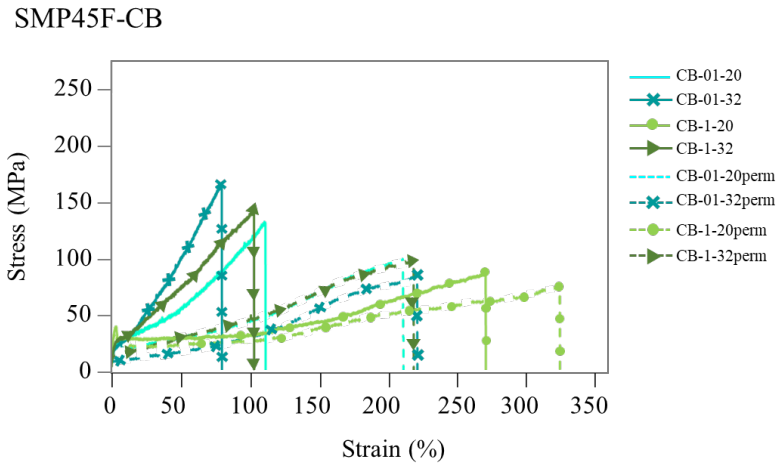

Figure 5. Stress–strain representative curves in static tensile tests of the SMPU filaments obtained on temporary shapes (solid colors) and on permanent shapes (stripes) for composite filaments with 0.1 and 1 wt.% of CB.

As can be seen in Figure 5, the addition of small amounts of CB leads to a significant increase of SMPU strain, in both temporary and permanent shapes. This could be related with a lubricant effect of the CB particles, their distribution into the polymer matrix and possible variation in diameter of the filaments (Table2), although more in depth studies should be done to analyze the effect of these particles. This behavior may be of interest for applications in which a high filament deformation in the permanent and temporary shapes is necessary. Table 5 presents the average maximum strength and strain values obtained from the curves.

Table 5. Maximum values of tensile strength and strain obtained for SMPU filaments with CB, 0.1 and 1 wt.%, on temporary and permanent shapes, from the tensile tests.

	TEMPORARY SHAPE		PERMANENT SHAPE	
SAMPLE NOMENCLATURE	**STRESS**	**STRAIN**	**STRESS**	**STRAIN**
Units	**(MPa)**	**(%)**	**(MPa)**	**(%)**
SMP45F-CB01-20	138 ±20	110 ±13	97 ±13	218 ±19
SMP45F-CB01-32	180 ±19	79 ±15	80 ±13	207 ±34
SMP45F-CB1-20	79 ±10	258 ±17	64 ±10	334 ±39

SMP45F-CB1-32	150 ±30	55 ±63	94 ±10	229 ±23

Thermal transitions and shape memory effect

The DSC curves corresponding to the 1st, 2nd and 3rd heating cycles for pure SMPU (as received), the composites (after preparing the masterbatch in the pellet form) and all of the materials forming the filaments, are presented in Figure 6 (temperature range from 30 to 60ºC). All of the curves revealed the typical transitions for SMPU polymers: the transition at low temperatures (approximately 45ºC) corresponding to the soft segment and the one at higher temperatures (approximately 160ºC) corresponding to the hard segment.[30]

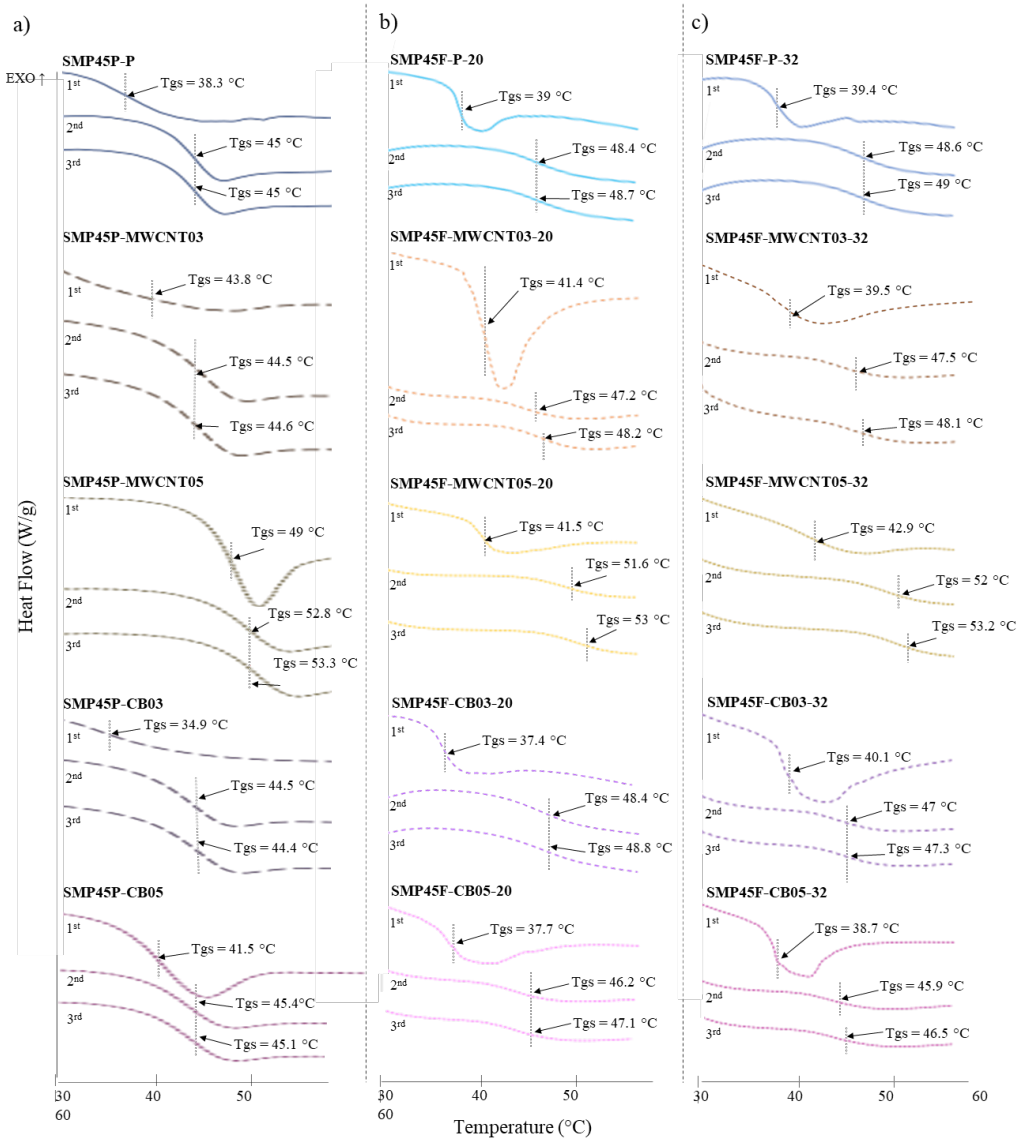

Figure 6. DSC curves of heating cycles for pure SMPU and the composites on pellet and filament from 30 to 60ºC. a) pellets; b) filament to 20 m/min drawing speed and c) filament to 32 m/min drawing speed.

Regarding the transition of the soft segment for all the samples (Figure 6) and comparison of the 3 heating cycles, lower T_{gs} were observed for all materials in the 1st heating (temporary shape) as compared to those from the 2nd and 3rd heating (permanent shape). This may be related to the stresses generated on the soft segments during the pellet to filament production[50] and the disappearance of these stresses after the first heating.

On the other hand, for the 2nd and 3rd heating, the production of filaments led to a slight increase in the T_{gs} which was more significant for higher drawing speeds, except for SMP45F-CB05-32. These results are in line with those of Sáenz-Pérez et al.[36], who found that the filaments had higher T_{gs} than the pellets, and Yang et al.[43], who found that SMPU experiences different T_{gs} under different programing and stress recovery conditions.

As for the effect of the additives on the T_{gs} of the 1st heating for the materials in pellet form (Figure 6a), slightly higher T_{gs} were observed for the composites as compared to the pure SMPU, except for the composite with 0.5 wt.% of MWCNT, which revealed a clear difference of up to 10ºC in the pellet form. This may have been due to the increased ordering of the chains in the extrusion process and the internal stresses generated from the stretching process.[3] In the 2nd and 3rd heating, however, a similar behavior was observed for all of the materials (with a T_{gs} around 45ºC) except for the composite with 0.5% MWCNT, with a T_{gs} of approximately 53ºC. A decrease in T_{gs} in the filaments composed of CB and an increase in T_{gs} in the compounds with MWCNT were observed in the study by Leng et al.,[10] although with higher amounts of additives.

For temperatures above the T_{gh}, a broad endothermic signal was observed in the first heating (between 120 and 180ºC), which disappeared over the successive cycles. This signal may be related to water desorption and/or tensions generated during the spinning process. During the 2nd and 3rd heating cycle, the signal's thickness was significantly reduced on the permanent shape of the filament. The enthalpy of the peak decreased on the 2nd and 3rd cycle, probably due to the fast crystallization process that did not permit the full reordering of this phase.[51–54]

As was previously explained, two types of DMA tests were performed to determine the shape memory effect (SME). From the first tests, the reference temperature (T_r) for the filaments drawn at 32 mm/min was determined to have the highest T_{gs} value. The T_{gs} obtained with DMA was higher than that determined from the DSC tests. This effect was attributed to a different type of heat transfer on the DMA (mainly through convection) as compared to the DSC (predominantly through conduction), offering greater precision to the DMA results.[36,55] As seen in Figure 7, a temperature of 90ºC ensured the total removal of residual stress in the soft segments of the temporary shape.

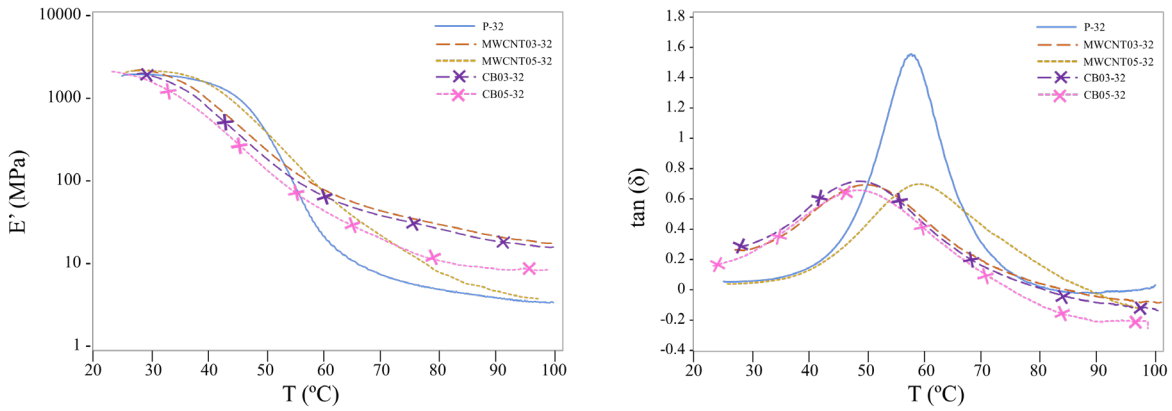

Figure 7. Comparison of dynamic mechanical analysis (DMA) curves of pure and composite SMPU.

This T_r was used to perform a cyclic tensile DMA test to determine the fixity ratio (R_f) and shape recovery ratio (R_r), erasing the residual stress in each cycle and creating the temporary shape. The curves obtained from the cyclic DMA test are presented in Figure 8.

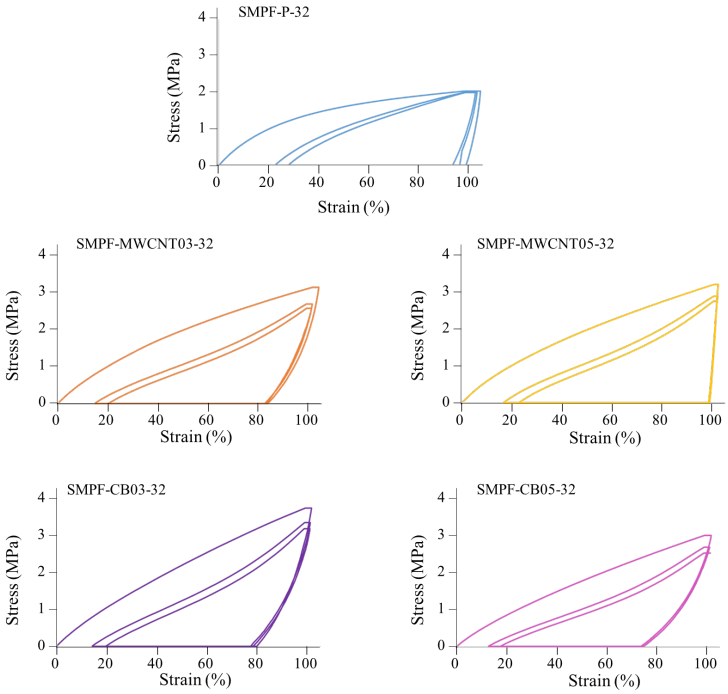

Figure 8. Stress-strain curves obtained from the cyclic DMA tensile test at T_r 90ºC for pure SMPU and composites.

As Figure 8 shows, the stress required for the filament deformation was lower for the pure SMPU than for the composites. This result contradicted that found for the static tensile testing carried out at room temperature. This may be due to the higher presence of soft segments on pure SMPU, as compared to the composites. These soft segments may be easily deformed since they have a rubbery state at the DMA test temperature.[42] This improved dynamic-mechanical resistance with the incorporation of additives has been found in other studies.[55]

As for the calculated fixity ratio (R_f), the highest value was found for the SMP45F-MWCNT05 (97%) composite, followed by the SMP45F-P composite (90%), the SMP45F-MWCNT03 composite (81%), and the CB composites (with 72 and 73% recovery for SMP45F-CB03 and SMP45F-CB05, respectively) (Table 6). The low fixity ratio, especially in the CB composites, could be due to the relationship between a lower initial temperature range of T_{gs} (see Figure 7) and the room temperature (27ºC) cooling used. Room temperature was selected since the study aims to source SMPU filaments for multi-sectorial uses such as those of the automotive, medical, technical clothing, apparel, and fabric sectors.

Table 6. Fixity and recovery ratio of cyclic DMA of pure and composite SMPU.

	C1

SAMPLE NOMENCLATURE	ε_m	ε_p	ε_u	R_f	R_r
SMP45F-P-32	107 ±0.2	18 ±3.4	96 ±1.5	**90 ±1.4**	**83 ±3.1**
SMP45F- MWCNT03-32	104 ±1.1	15 ±0.2	84 ±2.8	**81 ±3.5**	**86 ±0.1**
SMP45F- MWCNT05-32	102 ±0.2	18 ±0.6	98 ±0.5	**97 ±0.4**	**83 ±0.5**
SMP45F- CB03-32	103 ±0.2	15 ±1.3	75 ±3.7	**73 ±3.7**	**86 ±1.3**
SMP45F- CB05-32	103 ±0.1	15 ±1.5	74 ±3.7	**72 ±3.5**	**86 ±1.4**
			C2		
SMP45F-P-32	105 ±0.2	24 ±3.0	94 ±0.3	**89 ±0.4**	**77 ±2.8**
SMP45F- MWCNT03-32	102 ±0.1	20 ±0.2	83 ±3.2	**81 ±3.2**	**80 ±0.2**
SMP45F- MWCNT05-32	102 ±0.1	24 ±0.5	98 ±0.2	**96 ±0.3**	**77 ±0.5**
SMP45F- CB03-32	103 ±0.4	21 ±1.1	75 ±3.6	**73 ±3.3**	**80 ±1.0**
SMP45F- CB05-32	102 ±0.2	20 ±1.7	74 ±3.1	**72 ±3.0**	**80 ±1.6**
			C3		
SMP45F-P-32	104 ±0.3	27 ±2.8	91 ±2.4	**87 ±2.5**	**74 ±2.7**
SMP45F- MWCNT03-32	102 ±0.1	24 ±0.2	82 ±2.4	**80 ±2.4**	**77 ±0.2**
SMP45F- MWCNT05-32	102 ±0.1	27 ±0.5	98 ±0.7	**96 ±0.6**	**73 ±0.5**
SMP45F- CB03-32	103 ±0.2	24 ±1.0	75 ±3.7	**73 ±3.6**	**77 ±0.9**
SMP45F- CB05-32	102 ±0.1	21 ±4.5	75 ±3.1	**73 ±3.0**	**80 ±4.4**

The recovery ratio (R_r) was slightly higher in filaments with CB and MWCNT03, 86%, as compared to the other filaments studied. All filaments showed a reduction in the second and third cycle.

Regarding the thermal stability of the materials, the TGA and the DTA values obtained for the pure SMPU and the composites in the pellet form are shown in Table 7. It is generally accepted that thermal degradation in polyurethanes occurs in two or three steps, depending on the quantity of the polyols, diisocyanates, and chain extenders, as well as the chemical structure.[42] The fourth step corresponds to the onset of carbonization. Four degradation steps were clearly identified for both pure SMPU and composites.

Table 7 shows the maximum degradation temperature for these four steps, the initial decomposition temperatures ($Ti_{5\%}$), determined as the temperature at 5% weight loss and the wt.% residue.[36]

Table 7. Thermal degradation temperatures obtained from TGA/DTG curves for pure SMPU and composites.

	THERMAL DEGRADATION			
SAMPLE NOMENCLATURE	**$Ti_{5\%}$**	**$Tmax_1$**	**$Tmax_2$**	**$Tmax_3$**
Units	**ºC**	**ºC**	**ºC**	**ºC**
SMP45P - P	321	348	392	426
SMP45P - MWCNT03	322	350	387	439
SMP45P - MWCNT05	322	344	374	426
SMP45P - CB03	319	346	382	425
SMP45P - CB05	322	345	387	423

Initial weight loss began at 260ºC, as found in previous studies.[56] At 320ºC, weight loss reached 5%.[42] The first main degradation step occurred between 320ºC and 360ºC and the maximum degradation temperatures were identified at 348ºC ($Tmax_1$). The second main degradation step occurred from 360°C to 460ºC, peaking at 380ºC ($Tmax_2$). The

third main degradation step took place from 400°C to 460ºC, peaking at 430ºC ($Tmax_3$). According to Sáenz-Pérez[42], the first step of the weight loss is attributed to the decomposition of the urethane groups. The second step may be connected to the destruction of the ether groups and the third step is a result of the destruction of the carbon chains and rings.

No significant differences were found for the maximum thermal degradation temperatures of the different samples. Some authors, however, have found that differences were caused by the presence of high amounts of carbon nanotubes.[57] The low amounts present in the filaments in this study may justify a similar thermal behavior for the SMPU composites as compared to the pure material. In this sense, Moghim et al.[58] suggested that only percentages above 0.5 wt.% of CB cause changes in thermal stability.

These results suggest that additives do not have a significant effect on SMPU degradation. Moreover, it can be concluded that the melt spinning temperatures used were appropriate and that composites may be processed at similar temperatures as pure material.

Conclusions

The influence of carbon-based additives on SMPUs plays an increasingly important role in the industry. No studies have yet analyzed the influence of additive contents inferior to 1% on the mechanical and thermomechanical behavior of filament yarns.

The results of this study clearly indicate that it is possible to obtain SMPU-based filaments with controlled yarn count and thermo-mechanical behavior using a very low content (0.3 and 0.5 wt.%) of MWCNT and CB reinforcement. The melt spinning process was designed to generate the permanent and temporary shape during this extrusion process.

The results also revealed that it is possible to obtain different mechanical properties with additives, without considerably affecting the glass transition temperature (T_g), except for MWCNT05, which increased the T_g by up to 10ºC. However, depending on the desired SME (fixity and recovery ratio), MWCNT will be used for higher fixation or CB will be used for higher recovery.

This study offers a novel approach that may be used to obtain SMPU-based filament yarns with stimuli-responsiveness, specific tailored shape-memory properties and controlled physical and mechanical performances for multi-sectorial applications.

Declaration of conflicting interests

The author(s) declared no potential conflicts of interest with respect to the research, authorship, and/or publication of this article.

References

1. Juan YH, Wong YC, Wang LJ, et al. Characterization Methods for Shape-Memory Polymers. *Chinese J Radiol*

2009; 34: 253–261.
2. Hu J, Chen S. A review of actively moving polymers in textile applications. *J Mater Chem* 2010; 20: 3346–3355.
3. Meng Q, Hu J, Zhu Y. Shape-memory polyurethane/multiwalled carbon nanotube fibers. *J Appl Polym Sci* 2007; 106: 837–848.
4. Abdullah SA, Jumahat A, Abdullah NR, et al. Determination of shape fixity and shape recovery rate of carbon nanotube-filled shape memory polymer nanocomposites. *Procedia Eng* 2012; 41: 1641–1646.
5. Ratna D, Karger-Kocsis J. Recent advances in shape memory polymers and composites: A review. *J Mater Sci* 2008; 43: 254–269.
6. Gunes IS, Cao F, Jana SC. Evaluation of nanoparticulate fillers for development of shape memory polyurethane nanocomposites. *Polymer (Guildf)* 2008; 49: 2223–2234.
7. Luo H, Zhou X, Ma Y, et al. Shape memory-based tunable resistivity of polymer composites. *Appl Surf Sci* 2016; 363: 59–65.
8. Yong Zhu1, Jinlian Hu1*, Jing Lu1 LYY and KY, 1Institute. Shape memory fiber spun with segmented polyurethane ionomer. *Pharmacovigil Rev* 2018; 10: 8–11.
9. Meng Q, Hu J. A review of shape memory polymer composites and blends. *Composites Part A: Applied Science and Manufacturing* 2009; 40: 1661–1672.
10. Leng J, Lv H, Liu Y, et al. Synergic effect of carbon black and short carbon fiber on shape memory polymer actuation by electricity. *J Appl Phys* 2008; 104: 3–7.
11. Aslan S, Kaplan S. Thermomechanical and Shape Memory Performances of Thermo-sensitive Polyurethane Fibers. *Fibers Polym* 2018; 19: 272–280.
12. Kaursoin J, Agrawal AK. Melt spun thermoresponsive shape memory fibers based on polyurethanes: Effect of drawing and heat-setting on fiber morphology and properties. *J Appl Polym Sci* 2007; 103: 2172–2182.
13. Article R, Lei M, Chen Z, et al. Recent progress in shape memory polymer composites: methods , properties , applications and prospects. *Nanotechnol Rev* 2019; 8: 327–351.
14. Panahi-Sarmad M, Abrisham M, Noroozi M, et al. Deep focusing on the role of microstructures in shape memory properties of polymer composites: A critical review. *European Polymer Journal* 2019; 117: 280–303.
15. Vaithylingam R, Ansari MNM, Shanks RA. Recent Advances in Polyurethane-Based Nanocomposites: A Review. *Polym Plast Technol Eng* 2017; 56(14): 1528–1541.
16. Ponnamma D, Sadasivuni KK, Cabibihan JJ, et al. Smart Polymer Nanocomposites. *Springer Series on Polymer and Composite Materials* 2017; 95-118.
17. Triadji W, Dong Y, Pramanik A, et al. Smart polyurethane composites for 3D or 4D printing: General-purpose use, sustainability and shape memory effect. *Compos Part B* 2021; 223: 109104.
18. Mustapha KB, Metwalli KM. A review of fused deposition modelling for 3D printing of smart polymeric materials and composites. *Eur Polym J* 2021; 156: 110591.
19. Pradhan S, Kumar S, Pramanik J, et al. An insight into mechanical & thermal properties of shape memory polymer reinforced with nanofillers; a critical review. *Mater Today Proc* 2022; 50: 1107-1112.
20. Mu T, Liu L, Lan X, et al. Shape memory polymers for composites. *Compos Sci Technol* 2018; 160: 169–198.

21. Liu T, Zhou T, Yao Y, et al. Stimulus methods of multi-functional shape memory polymer nanocomposites: A review. *Compos Part A Appl Sci Manuf* 2017; 100: 20–30.
22. Lu H, Lei M, Yao Y, et al. Shape Memory Polymer Nanocomposites : Nano-Reinforcement and Multifunctionalization. *Nanosci Nanotechnol Lett* 2014; 6(9): 772–786.
23. Badamshina Elmira EY, Gafurova M. Nanocomposites based on polyurethanes and carbon nanoparticles: preparation , properties and application. *J Mater Chem A* 2013; 6509–6529.
24. Sahoo NG, Rana S, Cho JW, et al. Polymer nanocomposites based on functionalized carbon nanotubes. *Prog Polym Sci* 2010; 35: 837–867.
25. Akpan EI, Shen X, Wetzel B, et al. Design and Synthesis of Polymer Nanocomposites. *In Polymer composites with functionalized nanoparticles (pp. 47-83). Elsevier.* 2019; 47-83.
26. Qian MY, He JH. Collection of polymer bubble as a nanoscale membrane. *Surfaces and Interfaces* 2022; 28: 101665.
27. Wang L, Zhang F, Liu Y, et al. Shape Memory Polymer Fibers : Materials , Structures , and Applications. *Adv Fiber Mater*. Epub ahead of print 2021. DOI: 10.1007/s42765-021-00073-z.
28. Wan T, Stylios GK. Shape memory training for smart fabrics. *Trans Inst Meas Control* 2007; 29: 321–336.
29. Hasan SM, Nash LD, Maitland DJ. Porous shape memory polymers: Design and applications. *J Polym Sci Part B Polym Phys* 2016; 54: 1300–1318.
30. Ji FL, Zhu Y, Hu JL, et al. Smart polymer fibers with shape memory effect. *Smart Mater Struct* 2006; 15: 1547–1554.
31. Meng Q, Hu J. Influence of Heat Treatment on the Properties of Shape Memory Fibers. I. Crystallinity, Hydrogen Bonding, and Shape Memory Effect. *Journal of Applied Polymer Science* 2008; 109: 2616-2623.
32. Zhu Y, Hu J, Yeung LY, et al. Effect of steaming on shape memory polyurethane fibers with various hard segment contents. *Smart Mater Struct* 2007; 16: 969–981.
33. Zhu Y, Hu J, Yeung LY, et al. Development of shape memory polyurethane fiber with complete shape recoverability. *Smart Mater Struct* 2006; 15: 1385–1394.
34. Liu Y, Chung A, Hu J, et al. Shape memory behavior of SMPU knitted fabric. *J Zhejiang Univ Sci A* 2007; 8: 830–834.
35. Kumar B. Innovation in Compression Therapy for Chronic Venous Insufficiency – Smart Textile. *Ann Vasc Med Res* 2016; 3: 3–5.
36. Sáenz-Pérez M, Bashir T, Laza JM, et al. Novel shape-memory polyurethane fibers for textile applications. *Text Res J* 2018; 89: 1027–1037.
37. Liu Y, Lu J, Hu J, et al. Study on the bagging behavior of knitted fabrics by shape memory polyurethane fiber. *J Text Inst* 2013; 104: 1230–1236.
38. Erkmen B, Bayram G. Improvement in mechanical, electrical, and shape memory properties of the polystyrene-based carbon fiber-reinforced polymer composites containing carbon nanotubes. *J Appl Polym Sci* 2021; 138: 1–23.
39. Uranbey L, Unal HI, Calis G, et al. One-Pot Preparation of Electroactive Shape Memory Polyurethane / Carbon Black Blend. *J Mater Eng Perform* 2021; 30: 1665–1673.

40. Meng H, Li G. A review of stimuli-responsive shape memory polymer composites. *Polymer (Guildf)* 2013; 54: 2199–2221.
41. Meng Q, hu J, Zhu Y, et al. Biological Evaluations of a Smart Shape Memory Fabric. *Text Res J* 2009; 79: 1522–1533.
42. Sáenz-Pérez M, Laza JM, García-Barrasa J, et al. Influence of the soft segment nature on the thermomechanical behavior of shape memory polyurethanes. *Polym Eng Sci* 2018; 58: 238–244.
43. Yang Q, Li G. Investigation into stress recovery behavior of shape memory polyurethane fiber. *J Polym Sci Part B Polym Phys* 2014; 52: 1429–1440.
44. Lee SH, Kim JW, Kim BK. Shape memory polyurethanes having crosslinks in soft and hard segments. *Smart Mater Struct* 2004; 13: 1345–1350.
45. Weems AC, Raymond JE, Easley AD, et al. Shape memory polymers with visible and near-infrared imaging modalities: synthesis, characterization and in vitro analysis. *RSC Advances* 2017; 7: 19742–19753.
46. Miaudet P, Derre A, Maugey M, et al. Shape and Temperature Memory of Nanocomposites with Broadened Glass Transition. *Science (80-)* 2007; 318: 1294–1296.
47. Yuen MC, Bilodeau RA, Kramer RK. Active Variable Stiffness Fibers for Multifunctional Robotic Fabrics. *IEEE Robot Autom Lett* 2016; 1: 708–715.
48. Meng Q, Hu J, Zhu Y, et al. Polycaprolactone-Based Shape Memory Segmented Polyurethane Fiber. *J Appl Polym Sci* 2007; 106: 2515–2523.
49. Huang Y, Inomata N, Wang Z, et al. Flexible Porous Carbon Black – Polymer Composites with a High Gauge Factor. *Sensors Mater* 2020; 32: 2527–2538.
50. Hong SJ, Yu W, Youk JH, et al. Polyurethane Smart Fiber with Shape Memory Function: Experimental Characterization and Constitutive Modelling. *Fibers Polym* 2007; 8: 377–385.
51. Li G. Self-Healing Composites: Shape Memory Polymer Based Structures - Cap.:5 Shape Memory Polyurethane Fiber. *Self-Healing Compos Shape Mem Polym Based Struct* 2014; 9781118452: 1–370.
52. Meng Q, Hu J, Mondal S. Thermal sensitive shape recovery and mass transfer properties of polyurethane/modified MWNT composite membranes synthesized via in situ solution pre-polymerization. *J Memb Sci* 2008; 319: 102–110.
53. Liu F, Zhang T, He C-H, et al. Thermal oscillation arising in a heat shock of a porous hierarchy and its application. *Facta Univ Ser Mech Eng*. DOI: 10.22190/FUME210317054L
54. He JH, Abd Elazem NY. Insights into partial slips and temperature jumps of a nanofluid flow over a stretched or shrinking surface. *Energies* 2021; 14: 1–21.
55. Gracia-fernández CA, Gómez-barreiro S, López-beceiro J, et al. Comparative study of the dynamic glass transition temperature by DMA and TMDSC. *Polym Test* 2010; 29: 1002–1006.
56. Wu XL, Huang WM, Lu HB, et al. Characterization of polymeric shape memory materials. *J Polym Eng* 2017; 37: 1–20.
57. Lee HF, Yu HH. Study of electroactive shape memory polyurethane-carbon nanotube hybrids. *Soft Matter* 2011; 7: 3801–3807.
58. Moghim MH, Zebarjad SM, & Eqra R. Experimental and modeling investigation of shape memory behavior of

polyurethane / carbon nanotube nanocomposite. *Polym Adv Technol* 2018; 29: 2496–2504.